DTU Library

Sulfation of Condensed Potassium Chloride by SO2

Sengeløv, Louise With; Hansen, Troels Bruun; Bartolomé, Carmen; Wu, Hao; Pedersen, Kim H.; Jappe Frandsen, Flemming; Jensen, Anker Degn; Glarborg, Peter

Link back to DTU Orbit

Sulfation of Condensed Potassium Chloride by SO₂

Louise With Sengeløv,[†] Troels Bruun Hansen,[†] Carmen Bartolomé,[‡] Hao Wu,[†] Kim H. Pedersen,[§] Flemming J. Frandsen,[†] Anker D. Jensen,[†] and Peter Glarborg*,[†]

[†]Department of Chemical and Biochemical Engineering, Technical University of Denmark, DK-2800 Kgs. Lyngby, Denmark
[‡]CIRCE (Centre of Research for Energy Resources and Consumption), University of Zaragoza, C/Mariano Esquillor Gómez, 15, 50018 Zaragoza, Spain
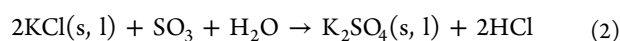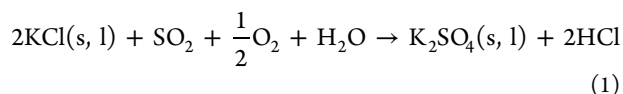[§]FLSmidth A/S, Vigerslev Allé 77, DK-2500 Valby, Denmark

ABSTRACT: The interaction between alkali chloride and sulfur oxides has important implications for deposition and corrosion in combustion of biomass. In the present study, the sulfation of particulate KCl (90−125 μm) by SO₂ was studied in a fixed bed reactor in the temperature range 673−1023 K and with reactant concentrations of 500−3000 ppm SO₂, 1−20% O₂, and 4−15% H₂O. The degree of sulfation was monitored by measuring the formation of HCl. Analysis of the solid residue confirmed that the reaction proceeds according to a shrinking core model and showed the formation of an eutectic at higher temperatures. On the basis of the experimental results, a rate expression for the sulfation reaction was derived. The model compared well with literature data for sulfation of KCl and NaCl, and the results indicate that it may be applied at even higher SO₂ concentrations and temperatures than those of the present study. Simulations of sulfation of KCl particles with different size indicate that only for very small KCl particles, below 1 μm, a considerable in-flight sulfation is achievable at the short gas residence times typical of combustion systems.

INTRODUCTION

The sulfation of alkali chlorides has important implications for thermal conversion of biomass. During pyrolysis and combustion of biomass at temperatures above about 1073 K, potassium is partly released to the gas-phase,[1−12] typically as potassium chloride. For agricultural residues, the KCl release can be significant,[3,4,11,13,14] while woody biomass contains smaller quantities of K and Cl.[8,9,13−16] Once released, gaseous KCl may be sulfated by reaction with SO₃[17−22] or it may, during cooling, condense on particulates or heat transfer surfaces.[18,23−26] If the particle loading in the system is low, KCl may form an aerosol by homogeneous nucleation.[24,25,27]

Potassium chloride has a number of adverse effects in combustion units. Once deposited on heat transfer surfaces, it may act to lower the melting temperature of the deposit, forming a sticky surface that promotes further deposition.[26,28] Furthermore, its presence in the deposits may lead to severe corrosion by a mechanism where both potassium and chlorine are active in destroying the metal oxide protective layer.[29] Another adverse effect of KCl is the ability to deactivate SCR catalysts;[30−33] a phenomenon that limits the application of SCR for NOₓ control in biomass fired systems.

The sulfation of condensed alkali chlorides proceeds as a gas−solid or gas−liquid reaction that may involve SO₂[34] or SO₃:[35]

$$2KCl(s, l) + SO_2 + \frac{1}{2}O_2 + H_2O \rightarrow K_2SO_4(s, l) + 2HCl \tag{1}$$

$$2KCl(s, l) + SO_3 + H_2O \rightarrow K_2SO_4(s, l) + 2HCl \tag{2}$$

Here s and l denote solid and liquid species, respectively, while the remaining species are gaseous. These reactions have been reported to be slower than the homogeneous sulfation occurring in the gas-phase,[17,36] leading to the assumption that the in-flight sulfation of particulate KCl is insignificant in a furnace where the residence time in suspension is of the order of a few seconds. However, for KCl condensed on deposits, the available reaction time for sulfation is orders of magnitude longer. Corrosion due to HCl release close to the metal surface is in discussion,[29,37−39] but recent results indicate that the sulfation reaction serves to reduce the corrosion propensity.[40]

In addition to its relevance for biomass combustion, the sulfation of alkali chlorides has implications for industrial production of HCl,[34] HCl emissions from municipal solid waste incinerators[41,42] and kraft recovery boilers,[43] as well as for corrosion of gas turbine engine components[35] and cement kilns.[44] Despite the importance, there are only few reported experiments on sulfation of solid alkali chlorides. Most previous studies investigated the sulfation of NaCl(s) by SO₂.[34,36] In more recent work, Matsuda and co-workers[45,46] compared the sulfation rates of NaCl(s), KCl(s), and CaCl₂(s). The reported experiments were typically conducted with a fixed bed of alkali chloride, varying temperature, and concentrations of SO₂, O₂, and H₂O. While these studies offer data for reaction rates and orders in reactants, results were mostly obtained for SO₂ concentrations of 3000 ppm and larger; i.e., considerably above the levels typically found in combustion systems. For this reason, rate coefficients may not extrapolate well to practical conditions.

The objective of the present work is to study the sulfation of condensed KCl by SO₂ in the temperature range 673−1023 K and lower SO₂ concentrations than in previous work.

Experiments are conducted in a fixed bed reactor with reactant levels of 500−3000 ppm SO_2, 1−20% O_2, and 4−15% H_2O, and the degree of sulfation monitored by measuring the formation of HCl. A rate expression for the sulfation reaction is derived and results are compared to data from literature.

■ EXPERIMENTAL SECTION

The experiments were conducted in a fixed bed quartz reactor,[51] with solid KCl placed on a porous quartz plate in an isothermal zone. A schematic of the reactor is shown in Figure 1. Reactant gases (SO_2, O_2,
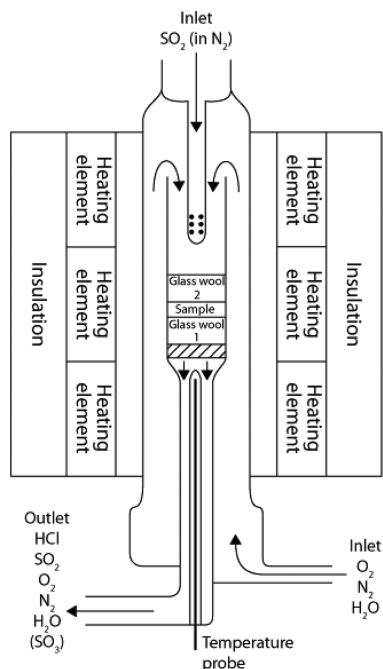

Figure 1. Schematic of the fixed bed reactor.

and H_2O in N_2) were introduced separately into the reactor and mixed just above the porous plate. The reactor temperatures were measured under inert conditions with a type K thermocouple (accuracy ±3 K). The temperature in the isothermal zone of the reactor was accurate within 10 K. The product gas was collected in the bottom part of the reactor and led to the online gas analyzers. Heated lines were used to avoid cold-spots where condensation could occur. The concentrations of HCl and SO_2 were measured continuously. The HCl analyzer (Servomex Servotough 2510) had an accuracy of ±1% of the measurement range (0−200 or 0−1000 ppm, depending on conditions). The exit concentration of SO_2 was measured with an analyzer accuracy of ±3%, but the possible adsorption of SO_2 onto tube surfaces contributes to the uncertainty for this species. In selected experiments, the KCl conversion to K_2SO_4 was quantified from analysis of the solid residue collected from the tests by ICP (inductively coupled plasma) spectroscopy. However, the uncertainty with the ICP analysis was considerable, partly due to difficulties in separating the sample from the quartz wool.

The experiments were conducted with commercial solid potassium chloride (purity 99.5%), and a mixture of SO_2, O_2, and N_2 from gas cylinders. Water vapor was added by saturating a nitrogen stream. The KCl was prepared by grinding and sieving to obtain a size range of 90−125 μm. A 1 g portion of sample material was used for each experiment. The KCl sample was placed in between two layers of quartz wool to limit loss of solid or molten material.

After placing the KCl sample inside the quartz reactor, it was exposed to N_2 for 30 min to allow the temperature to reach the desired value. Then the N_2 was replaced with a mixture of O_2, SO_2, H_2O, and N_2 (total gas flow of 1000 mL min^{-1} STP). After 1 h of sulfation, the reactant gas was replaced by inert. The mass of the water bottle was

determined, and the flows were checked to ensure that they did not deviate significantly from the set-point values.

During experiments, the reactor pressure was about 1.05 atm, varying slightly depending on the packing of the fixed bed. In the results discussed in the present work, the progress of reaction was based on the measurement of the exit concentration of HCl from the reactor. The measured consumption of SO_2 corresponded well to the formation of HCl. Reaction rates based on analysis of the solid residue collected from the tests were in reasonable agreement with data obtained from HCl detection but involved a significantly larger uncertainty.

Residual particles, collected from selected experiments, were sectioned and analyzed by SEM-EDS (scanning electron microscopy and electron dispersive X-rays spectroscopy). Furthermore, the fixed experiments were supplemented with results obtained from simultaneous thermal analysis (STA) with a heating rate of 5 K min^{-1}.

■ NUMERICAL PROCEDURE

Following the work of Matsuda et al.,[46] the reaction rate was defined as dX/dt, where X is the fractional conversion of KCl. X is defined as

$$X = \frac{m_0 - m}{m_0} \tag{3}$$

where m_0 (kg) is the initial mass of the KCl particle and m (kg) is the mass of the remaining unconverted KCl particle. For each experiment, dX/dt was determined from equation (4):

$$\frac{dX}{dt} = \dot{V}[\text{HCl}]\frac{MW_{KCl}}{m_{KCl}} \tag{4}$$

Here $\dot{V}$ (m^3 s^{-1}) is the total gas flow, $[\text{HCl}]$ (mol m^{-3}) is the peak concentration of HCl, MW_{KCl} (kg mol^{-1}) is the molecular weight of KCl, and m_{KCl} (kg) is the initial sample mass of KCl.

In the interpretation of the data, it is assumed that the particle is spherical and converted according to an unreacted shrinking core model under chemical reaction control. The assumption of a shrinking core model is based on the results reported by van Lith et al.[39] Further support is provided by the SEM-EDS analysis of the residual particles in the present work, as discussed below. Mass transfer limitations in the gas-film or the product layer are neglected, since the particles are small and since the rate is determined at low conversions of KCl.

With the assumption of a shrinking core model, the rate of conversion is given as

$$\frac{dX}{dt} = k'(1 - X)^{2/3}F(Y_{SO_2}, Y_{O_2}, Y_{H_2O}) \tag{5}$$

Here, the rate constant k' (s^{-1}), in Arrhenius form, describes the temperature dependence and F describes the functional dependence on the reactant mole fractions (Y_i).

Two formulations of the rate expression were used to analyze the experimental results. The first equation is similar to the one used by Matsuda et al.:[46]

$$\frac{dX}{dt} = k_A(1 - X)^{2/3}(Y_{SO_2})^1(Y_{O_2})^m(Y_{H_2O})^n \tag{6}$$

In the second formulation, we employ a Langmuir−Hinshelwood expression to describe the dependence on the SO_2 concentration:

$$\frac{dX}{dt} = k_B(1 - X)^{2/3}\frac{Y_{SO_2}}{1 + KY_{SO_2}}(Y_{O_2})^m(Y_{H_2O})^n \tag{7}$$

Equations 6 and 7 are only valid for the specific particle size R_0 used in the experiments. To predict the sulfation rate for other particle sizes, we derive a surface area based rate constant k'_s (kg m^{-2} s^{-1}), which is assumed to be universal for particles of difference size. Substitution of eq 3 for X into eq 5 yields

$$\frac{dm}{dt} = -k'm_0\left(\frac{m}{m_0}\right)^{2/3}F(Y_{SO_2}, Y_{O_2}, Y_{H_2O}) \tag{8}$$

For a spherical particle, the equation above can be converted to

$$\frac{dm}{dt} = -k'\frac{1}{3}R\rho_{KCl}4\pi r^2 F(Y_{SO_2}, Y_{O_2}, Y_{H_2O}) \tag{9}$$

where R (m) is the initial radius of the particle, ρ_{KCl} (kg m^{-3}) is the density of the KCl particle, and r (m) is the radius of the remaining unconverted particle. From eq 9, the surface area based rate constant k'_s can be obtained:

$$k'_s = k'\frac{1}{3}R\rho_{KCl} \tag{10}$$

Since eq 10 is assumed valid for all particle sizes, the conversion-based rate constant k_1 (s^{-1}) for a particle with an initial radius of R_1 can be calculated as

$$k'_1 = k'\frac{R_0}{R_1} \tag{11}$$

In the present study, the diameters of the KCl particles were in the range 90−125 μm. By assuming an equal mass distribution (with an interval of 1 μm) of the particles in this size range, we calculate a harmonic mean radius R_0 of 53.2 μm.

■ RESULTS AND DISCUSSION

Experiments on sulfation of solid KCl were conducted, varying temperature (673−1023 K) and reactant concentrations (500−3000 ppm SO$_2$, 1−20% O$_2$, 4−15% H$_2$O). All reported concentrations are volume based and on a wet basis. In the following, the effect of temperature and gas composition on the sulfation rate is investigated. On the basis of these data, a model for the rate of sulfation is established and compared with results from the literature.

Effect of Temperature. For the baseline gas composition (959−965 ppm SO$_2$, 4.8% O$_2$, 3.9−4.6% H$_2$O, balance N$_2$), the temperature was varied in the range 673−1023 K. Figure 2 shows the measured HCl profiles for the different temperatures.

At the lowest temperatures, the amount of HCl generated is comparatively small and the reaction rate derived is more uncertain. Above 900 K, the formation of HCl increases rapidly with temperature. At 1023 K, a second peak in HCl is observed after approximately 2500 s reaction time, indicating a sudden increase in the reaction rate. We attribute this phenomenon to a phase transition from a solid to a melt, likely due to the formation of an eutectic mixture of KCl and K$_2$SO$_4$. The melting is supported by the detection of an increased pressure in the reactor, caused by blocking of the pores in the quartz plate by the molten phase.

To confirm that a KCl−K$_2$SO$_4$ eutectic was formed during the experiments at 1023 K, the collected residual particles were sectioned and analyzed by SEM-EDS. Typical results are presented in Figure 3, where a mixture of KCl−K$_2$SO$_4$ with a lamellar structure is observed. Such a regular lamellar structure is a characteristic microstructure of an eutectic,[52,53] strongly supporting the presence of a KCl−K$_2$SO$_4$ eutectic under the
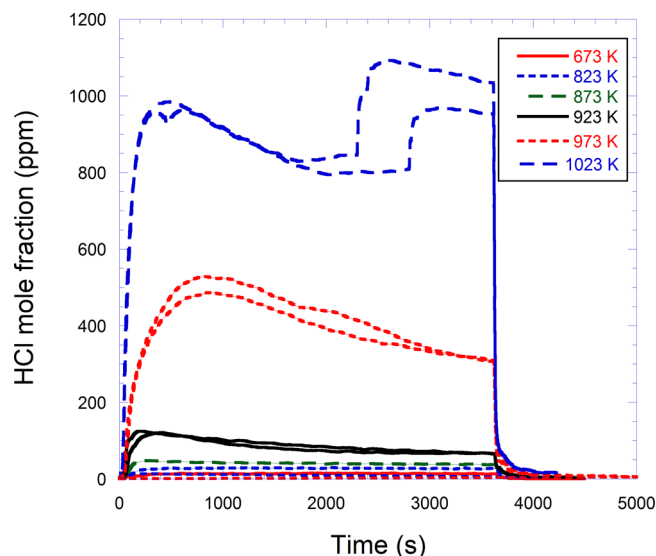

Figure 2. Measured HCl concentrations as a function of temperature and reaction time. Temperature 673−1023 K; gas composition 959−965 ppm SO$_2$, 4.8% O$_2$, 3.9−4.6% H$_2$O, balance N$_2$.
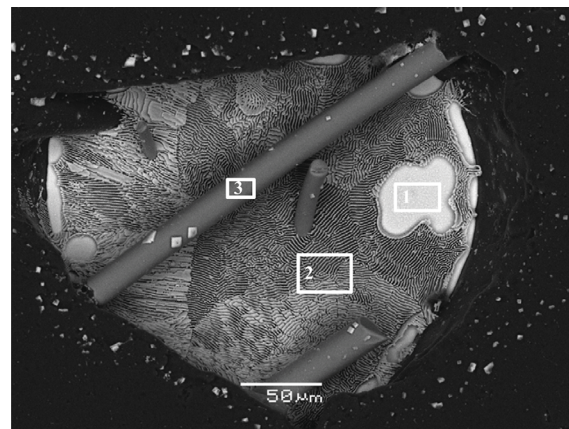

Figure 3. SEM (backscattered electrons, acceleration voltage 15 kW) image of the sectioned residual particles collected from the KCl sulfation experiment at 1023 K, with the selected areas comprised of (1) KCl; (2) a mixture of KCl−K$_2$SO$_4$ with a molar ratio of about 1:2.1; (3) SiO$_2$ (quartz wool used in the experiment).

given experimental conditions. The formation of a eutectic has been reported earlier by Fielder et al.[35] in sulfation of NaCl(s) by SO$_3$ above 900 K. Matsuda et al.[46] reported eutectic formation in sulfation of CaCl$_2$ but not for KCl or NaCl. The SEM-EDS analysis also shows that the core of the KCl particles is unreacted and that the sulfation reaction takes place on the surface. These results supports the assumption of a shrinking core model.

Figure 4 shows an Arrhenius plot of the sulfation reaction. It is evident that a change in reaction mechanism takes place between 823 and 873 K, in agreement with observations in the literature for KCl, NaCl, and CaCl$_2$.[45,46] In the present study, the activation energy for the high-temperature mechanism is determined to be 157 kJ mol^{-1}, in good agreement with the values of 137 (KCl) and 144 kJ mol^{-1} (NaCl) reported by Matsuda and co-workers,[45,46] but somewhat higher than the 115 kJ mol^{-1} derived for NaCl by Henriksson and Warnqvist.[34] Due to the small number of data points in the 623−873 K range and the limited experimental accuracy at low HCl
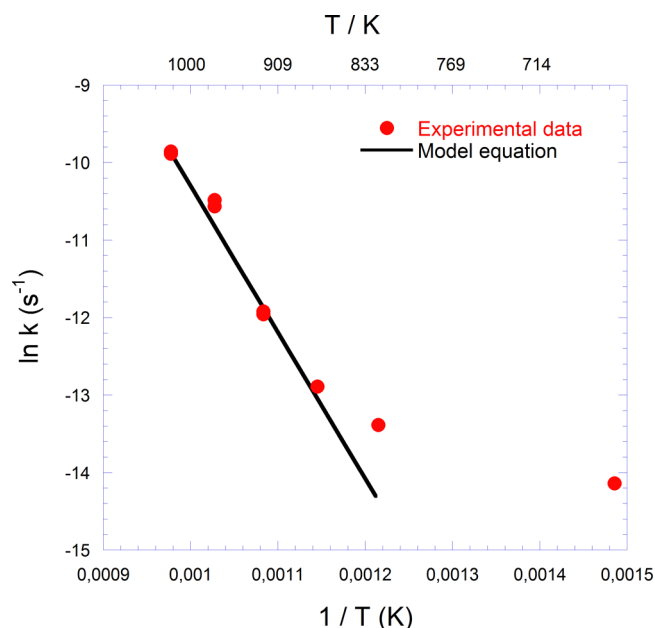
Figure 4. Arrhenius plot for the rate constant of sulfation of KCl and NaCl with SO_2. Temperature 673−1023 K; gas composition 959−965 ppm SO_2, 4.8% O_2, 3.9−4.6% H_2O, balance N_2.

Effect of Reactant Concentrations. A range of experiments were conducted at 923 K to determine the dependence of the sulfation rate on the concentrations of SO_2, O_2, and H_2O. Figure 5 shows results for variation of the SO_2
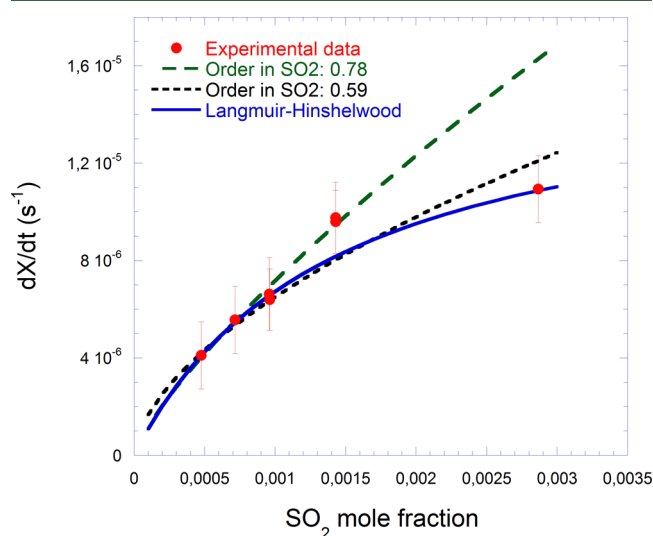

Figure 5. Comparison between the measured and calculated value of dX/dt as a function of SO_2 concentration. Temperature 923 K; gas composition 500−3000 ppm SO_2, 4.8% O_2, 4.0−4.6% H_2O, balance N_2.

concentrations, we cannot reliably determine the activation energy for the low-temperature mechanism, but our results are consistent with values of 3.4−23 kJ mol^{-1} reported for KCl and NaCl.[36,45,46]

The reason for the observed change in mechanism is still unresolved. Results from simultaneous thermal analysis (STA) for KCl indicated a phase transition of KCl around 1058 K, but no change in the crystal form of KCl was observed in the temperature range 823−923 K. Potassium sulfate exhibited a reversible change in crystal form at around 860 K, in agreement with literature reports,[47,48] but the enthalpy of transformation is only about 5.8 kJ mol^{-1} [48] and cannot in itself explain the change in activation energy of the sulfation reaction.

A plausible explanation to the observed change of mechanism is that the sulfation at low temperatures involves a condensed-phase intermediate, perhaps a potassium sulfite, with reduced thermal stability at temperatures above 900 K. Another possibility is that the low-temperature reaction involves SO_3, rather than SO_2, as reactant. The reaction between KCl(s,l) and SO_3 has been shown to proceed essentially without an activation energy.[35] Even though quartz is not very effective as a catalyst for SO_2 oxidation,[49] its presence (wool bed, reactor surface) may facilitate formation of SO_3 in quantities sufficient to explain the observed (small) conversion. A mechanism that involves surface oxidation of SO_2 would also help to explain the large scatter in reported sulfation rates in the 600−900 K range (see below).

It should be noted that the sulfation products at low temperatures (e.g., 673 K) may be dominated by potassium pyrosulfate ($K_2S_2O_7$), which is thermodynamically favored compared to K_2SO_4 under these conditions.[50] For both SO_2 and SO_3 as reactants, the formation of $K_2S_2O_7$ is exothermic. When the temperature is increased to a range of 823−873 K, decomposition of $K_2S_2O_7$ to SO_3 + K_2SO_4 (α or β phase) becomes important. This reaction is endothermic, with calculated reaction enthalpies of 65−75 kJ mol^{-1}.[50]

concentration, maintaining the concentrations of O_2 and H_2O at constant levels. A regression for the range 500−1500 ppm SO_2 is consistent with a $(Y_{SO_2})^{0.78}$ dependence (shown as the long-dashed line). As the SO_2 concentration is increased further (3000 ppm), the reaction order in SO_2 appears to decrease, possibly due to a saturation in SO_2 when adsorbing on the surface. Over the range 500−3000 ppm, the best fit is obtained with $(Y_{SO_2})^{0.59}$ (short-dashed line). These values can be compared with a reaction order of 0.5, obtained for the range 3000−13000 ppm SO_2 by Matsuda et al.[46] An alternative to a power fit is the Langmuir−Hinshelwood type expression (eq 7) of the type $Y_{SO_2}/(1 + KY_{SO_2})$ (shown as a solid line for $K = 708$), which may provide a more accurate extrapolation to higher concentrations of SO_2.

Figure 6 shows results for variation of O_2. These data, obtained over a wide range of O_2 concentrations (1−20%), are consistent with a reaction order of 0.37, in good agreement with the value of 0.4, obtained for the range 2.5−15% O_2 by Matsuda et al.[46] The water vapor level was varied between 4.3 and 15% (Figure 7). The water concentration was more difficult to control and to quantify than the other reactant concentrations, but our results show only little sensitivity of the sulfation rate toward H_2O in the investigated range. A best fit to the data yields a reaction order in H_2O of 0.15, but within the uncertainty of the data, the sulfation rate can be assumed independent of [H_2O]. The results obtained by Matsuda et al.[46] indicate that above 923 K the water vapor level (5−20%) has a larger impact on the sulfation rate, but this cannot be verified from the present work.

Rate Expression for KCl Sulfation. On the basis of the experimental data, we have determined the sulfation rate as a function of temperature (873−1023 K) and reactant concentrations as follows. For SO_2 concentrations of 500−1500 ppm, the eq 6 format works well and we get
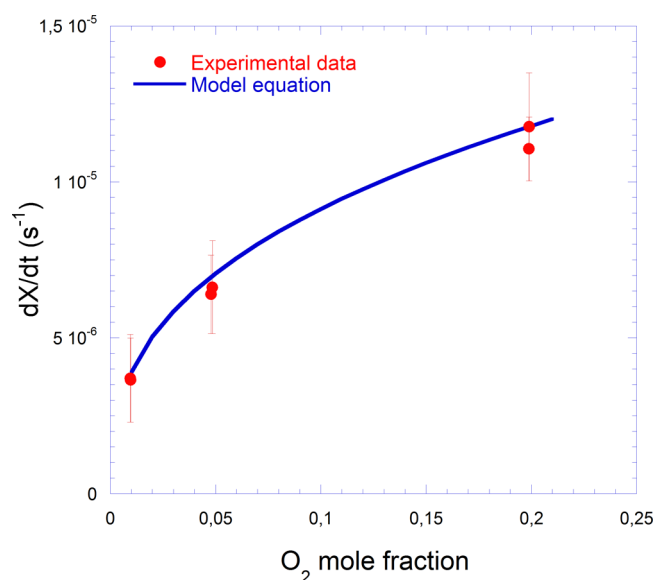
Figure 6. Comparison between the measured and calculated value of dX/dt as a function of O_2 concentration. Temperature 923 K; gas composition 959−968 ppm SO_2, 1.0−19.9% O_2, 3.8−4.6% H_2O, balance N_2.
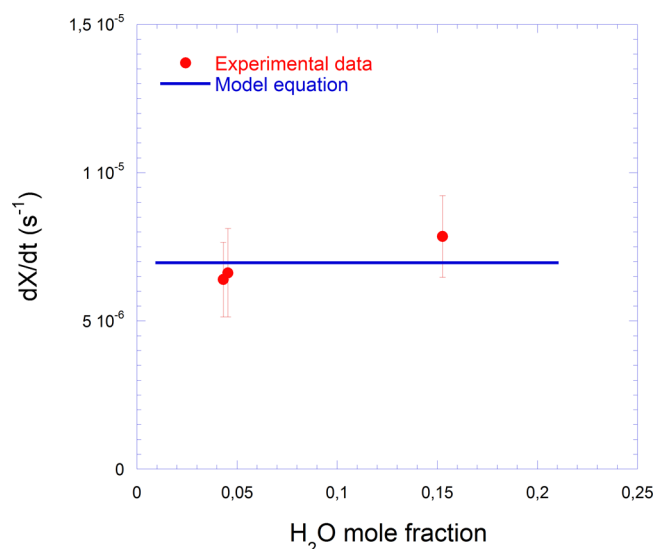

Figure 7. Comparison between the measured and calculated value of dX/dt as a function of H_2O concentration. Temperature 923 K; gas composition 947−962 ppm SO_2, 4.8% O_2, 4.3−15.3% H_2O, balance N_2.

$$\frac{dX}{dt} = 3.7 \times 10^6 \exp(-18900/T)(1 - X)^{2/3}(Y_{SO_2})^{0.78}$$
$$(Y_{O_2})^{0.37} \tag{12}$$

For a wider range of SO_2 concentrations, we recommend the eq 7 format with the following parameters:

$$\frac{dX}{dt} = 2.7 \times 10^7 \exp(-18900/T)(1 - X)^{2/3}\frac{Y_{SO_2}}{1 + 708Y_{SO_2}}$$
$$(Y_{O_2})^{0.37} \tag{13}$$

The Arrhenius plot in Figure 8 compares the present results with data from the work of Boonsongsup et al.[36] for NaCl and
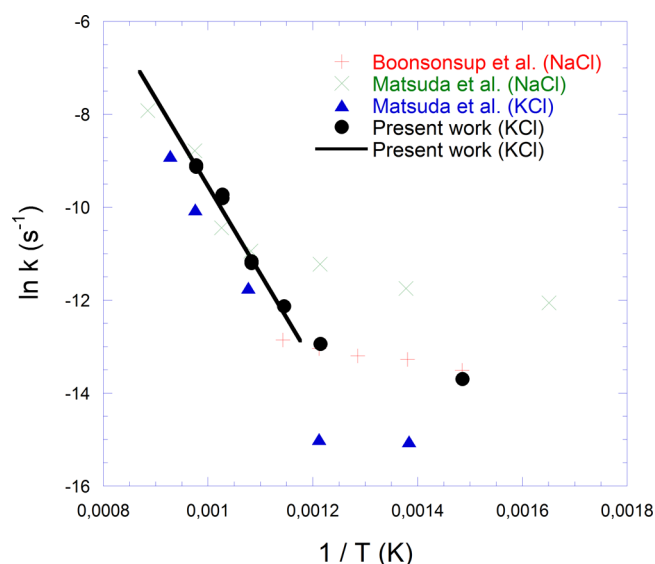

Figure 8. Arrhenius plot for the rate constant of sulfation of KCl and NaCl with SO_2. Nominal conditions for the comparison: SO_2 9000 ppm; O_2 5.0%; H_2O 10%; N_2 balance. Literature data is from Boonsongsup et al.[36] for NaCl and Matsuda et al.[46] for NaCl and KCl. The present data for KCl were obtained at conditions with 959−965 ppm SO_2, 4.8% O_2, and 3.9−4.6% H_2O. To extrapolate to the conditions of the figure, SO_2 was corrected according to the Langmuir−Hinshelwood expression (high temperature) and to $(P_{SO_2})^{0.2}$ (low temperature[46]), respectively, while no corrections were made for O_2 and H_2O.

Matsuda et al.[46] for NaCl and KCl. The comparison is complicated by the fact that the measurements were conducted in different SO_2 concentration ranges. The data shown in the figure by Boonsongsup et al. and by Matsuda et al. were obtained at 9000 ppm SO_2, while in the present work the SO_2 range was 500−3000 ppm. We extrapolate our results to the higher SO_2 level using the Langmuir−Hinshelwood formulation (eq 13) for the high temperature range (873−1023 K). The two data points obtained at the lowest temperatures were corrected using the $(P_{SO_2})^{0.2}$ dependence reported by Matsuda et al.[46]

The data for the sulfation rate of KCl and NaCl obtained by Matsuda et al.[46] above 873 K are in good agreement with the results of the present work. Our rate constant for KCl is slightly higher than that reported by Matsuda et al., perhaps because their value is derived for longer reaction times, where product layer diffusion may have affected the sulfation rate. For the low temperature regime, the scatter in the data is significantly larger. Our results are in good agreement with those reported by Boonsongsup et al. and in between data reported by Matsuda et al. for KCl and NaCl, respectively.

Extrapolation to Higher Temperatures. In order to evaluate how well the model extrapolates to higher temperatures, predictions were compared to data reported by Iisa et al.[17] They studied sulfation of KCl particles (65−125 μm) at temperatures of 1173−1373 K in an entrained flow reactor. At these temperatures, a significant fraction of the KCl evaporates to the gas phase, and three mechanisms of sulfation may be active:

(A) Sulfation of particulate KCl by reaction with SO_2
(B) Sulfation of particulate KCl by reaction with SO_3
(C) Sulfation of gaseous KCl by reaction with SO_3

Part of the inlet SO_2 may be oxidized homogeneously to SO_3, and the presence of SO_3 increases the sulfation rate of both particulate KCl^{35} (mechanism B) and gaseous $KCl^{17,19-22}$ (mechanism C) considerably. Iisa et al. analyzed both the coarse particles collected in the cyclone and the fine particles captured in the filter; from these data they determined the degree of sulfation of both particulate and gaseous KCl.

The results reported by Iisa et al. indicate an accelerated sulfation rate of the particulate KCl at longer residence times in the reactor. We attribute this mostly to interference from mechanisms B and C. Potassium sulfate, formed in the gas-phase (C), may condense on the coarse KCl particles, and also reaction of KCl(s) with SO_3 (B) may have contributed to the observed degree of sulfation. The B and C sulfation mechanisms are both controlled by the rate of SO_3 formation in the gas-phase. If they were important for the observed sulfation degree of solid KCl particles, the homogeneous and heterogeneous sulfation rates should be similar. Indeed, this is in agreement with the observations of Iisa et al. for longer reactor residence times (>1 s).

Iisa et al.[17] reported the sulfation degree of particulate KCl as a function of temperature and reactor residence time. Figure 9
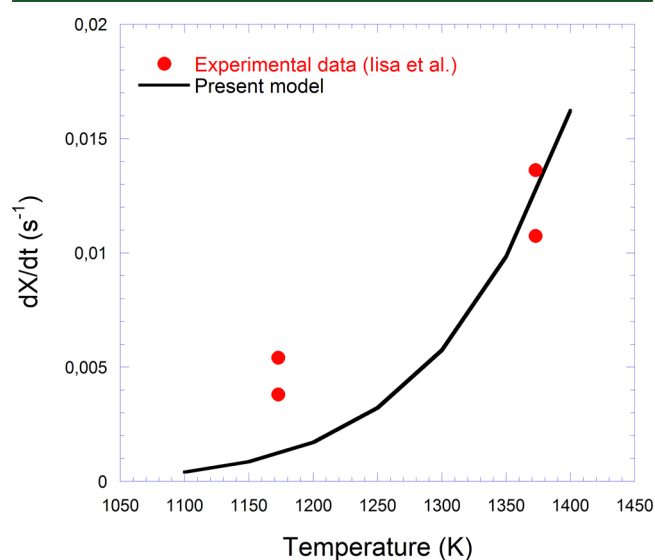

Figure 9. Comparison between measured and calculated values of dX/dt as a function of temperature. The experimental data are drawn from the entrained flow reactor work of Iisa et al.[17] while the calculated values are obtained from eq 13. Temperatures 1173 K (residence time 1.0 s) and 1373 K (residence time 0.6 s); gas composition 2% SO_2, 5% O_2, 10% H_2O; N_2 balance.

compares dX/dt values derived from these data with predictions using eq 13. Unfortunately, data for short residence times were only reported for a temperature of 1373 K (0.6 s). The data shown for 1173 K were obtained for a residence time of 1.0 s, and they are more prone to be influenced by mechanisms B and C, since SO_3 has had more time to form. Considering the uncertainty, the level of agreement between the entrained flow reactor data and the model is satisfactory.

In-Flight Sulfation of Particulate KCl. To assess the extent of in-flight sulfation of particulate KCl, the conversion has been calculated for different particle sizes and temperatures. The calculations were based on eq 13, correcting for the effect of particle radius following eq 11:

$$\frac{dX}{dt} = 2.7 \times 10^7 \exp(-18900/T)(1-X)^{2/3} \frac{Y_{SO_2}}{1 + 708 Y_{SO_2}}$$

$$(Y_{O_2})^{0.37} \frac{R_0}{R_1} \tag{14}$$

Here, R_0 is 53.2 μm; the harmonic mean diameter of the particle size range (90−125 μm) used in deriving the kinetic parameters.

The results are shown in Figure 10, which are obtained based on a gas mixture with 1000 ppm SO_2 and 5% O_2, and a
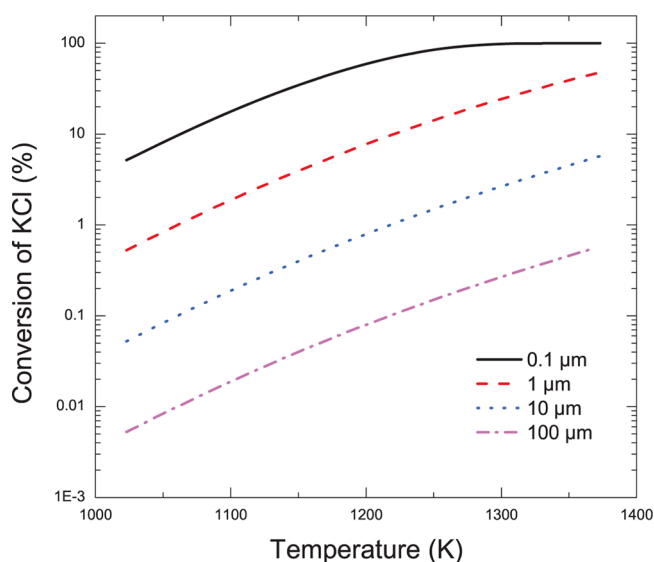

Figure 10. Calculated conversion (%) of KCl particles under different size and temperature conditions by using eq 14. The calculations are based on 1000 ppm SO_2, 5% O_2, and a residence time of 1 s.

residence time of 1 s. It can be seen that only for very small KCl particles (0.1−1 μm), a considerable in-flight conversion (in the range 1−100%) can be achieved. However, KCl aerosols, from homogeneous nucleation (at low particle loadings) or from heterogeneous condensation on K_2SO_4 nuclei, are unlikely to form at temperatures above 1100 K.[22] At temperatures below this value, the conversion of the submicrometer particles is limited to below 20%. For particles with diameters larger than 10 μm, the conversion is only a few percent even at very high temperatures. These results indicate that in-flight sulfation of particulate KCl in combustion systems is limited, in agreement with earlier findings.[17,36]

■ CONCLUSIONS

The sulfation of condensed KCl by SO_2 was studied in the temperature range 673−1023 K and with reactant concentrations of 500−3000 ppm SO_2, 1−20% O_2, and 4−15% H_2O. Experiments were conducted in a fixed bed reactor, and the degree of sulfation monitored by measuring the formation of HCl and analysis of the solid residue. On the basis of the experimental results, the rate of the sulfation reaction can be described by the expression $dX/dt = 2.7 \times 10^7 \exp(-18900/T)(1-X)^{2/3}[Y_{SO_2}/(1 + 708Y_{SO_2})](Y_{O_2})^{0.37}$ for particles in the range 90−125 μm. The model compares well with literature data for sulfation of KCl and NaCl, and the results indicate that it may be applied even at higher SO_2 concentrations and temperatures than those of the present study. Simulations of

the condensed phase sulfation of KCl particles with different size indicate that a considerable in-flight sulfation may be achieved only for KCl particles below 1 μm in combustion systems.

■ AUTHOR INFORMATION

Corresponding Author
*E-mail: pgl@kt.dtu.dk.

Notes
The authors declare no competing financial interest.

■ ACKNOWLEDGMENTS

■ REFERENCES

(1) Olsson, J. G.; Jaglid, U.; Pettersson, J. B. C.; Hald, P. *Energy Fuels* **1997**, *11*, 779−784.

(2) Björkman, E.; Strömberg, B. *Energy Fuels* **1997**, *11*, 1026−1032.

(3) Knudsen, J. N.; Jensen, P. A.; Lin, W.; Frandsen, F. J.; Dam-Johansen, K. *Energy Fuels* **2004**, *18*, 810−819.

(4) Knudsen, J. N.; Jensen, P. A.; Dam-Johansen, K. *Energy Fuels* **2004**, *18*, 1385−1399.

(5) Knudsen, J. N.; Jensen, P. A.; Lin, W.; Dam-Johansen, K. *Energy Fuels* **2005**, *19*, 606−617.

(6) Keown, D. M.; Favas, G.; Hayashi, J.; Li, C.-Z. *Biores. Technol.* **2005**, *96*, 1570−1577.

(7) Okuno, T.; Sonoyama, N.; Hayashi, J.-I.; Li, C.-Z.; Sathe, C.; Chiba, T. *Energy Fuels* **2005**, *19*, 2164−2171.

(8) van Lith, S. C.; Ramirez, V. A.; Jensen, P. A.; Frandsen, F. J.; Glarborg, P. *Energy Fuels* **2006**, *20*, 964−978.

(9) van Lith, S. C.; Jensen, P. A.; Frandsen, F. J.; Glarborg, P. *Energy Fuels* **2008**, *22*, 1598−1609.

(10) Tillman, D. A.; Duong, D.; Miller, B. *Energy Fuels* **2009**, *23*, 3379−3391.

(11) Johansen, J. M.; Jakobsen, J. G.; Frandsen, F. J.; Glarborg, P. *Energy Fuels* **2011**, *25*, 4961−4971.

(12) Zhang, Z.-H.; Song, Q.; Yao, Q.; Yang, R.-M. *Energy Fuels* **2012**, *26*, 1892−1899.

(13) Boström, D.; Skoglund, N.; Grimm, A.; Boman, C.; Öhman, M.; Broström, M.; Backman, R. *Energy Fuels* **2012**, *26*, 85−93.

(14) Zevenhoven, M.; Yrjas, P.; Skrifvars, B.-J.; Hupa, M. *Energy Fuels* **2012**, *26*, 6366−6386.

(15) Jenkins, B. M.; Baxter, L. L.; Miles, T. R., Jr.; Miles, T. R. *Fuel Process. Technol.* **1998**, *54*, 17−46.

(16) Coda, B.; Aho, M.; Berger, R.; Hein, K. R. G. *Energy Fuels* **2001**, *15*, 680−690.

(17) Iisa, K.; Lu, Y.; Salmenoja, K. *Energy Fuels* **1999**, *13*, 1184−1190.

(18) Jimenez, S.; Ballester, J. *Combust. Flame* **2005**, *140*, 346−358.

(19) Glarborg, P.; Marshall, P. *Combust. Flame* **2005**, *141*, 22−39.

(20) Jimenez, S.; Ballester, J. *Fuel* **2007**, *86*, 486−493.

(21) Hindiyarti, L.; Frandsen, F. J.; Livbjerg, H.; Glarborg, P.; Marshall, P. *Fuel* **2008**, *87*, 1591−1600.

(22) Li, B.; Sun, Z.; Li, Z.; Alden, M.; Jakobsen, J. G.; Hansen, S.; Glarborg, P. *Combust. Flame* **2013**, *160*, 959−969.

(23) Christensen, K. A.; Stenholm, M.; Livbjerg, H. *Aerosol Sci. Technol.* **1998**, *29*, 421−444.

(24) Christensen, K. A.; Livbjerg, H. *Aerosol Sci. Technol.* **2000**, *33*, 470−489.

(25) Jensen, J. R.; Nielsen, L. B.; Schultz-Moller, C.; Wedel, S.; Livbjerg, H. *Aerosol Sci. Technol.* **2000**, *33*, 490−509.

(26) Nielsen, H. P.; Baxter, L. L.; Sclippa, G.; Morey, C.; Frandsen, F. J.; Dam-Johansen, K. *Fuel* **2000**, *79*, 131−139.

(27) Zeuthen, J. H.; Jensen, P. A.; Jensen, J. R.; Livbjerg, H. *Energy Fuels* **2007**, *21*, 699−709.

(28) Frandsen, F. J. *Fuel* **2005**, *84*, 1277−1294.

(29) Karlsson, S.; Pettersson, J.; Johansson, L. G.; Svensson, J. E. *Oxid. Metals* **2012**, *78*, 83−102.

(30) Zheng, Y. J.; Jensen, A. D.; Johnsson, J. E. *Appl. Cat. B Env.* **2005**, *60*, 253−264.

(31) Larsson, A. C.; Einvall, J.; Andersson, A.; Sanati, M. *Energy Fuels* **2006**, *20*, 1398−1405.

(32) Kling, A.; Andersson, C.; Myringer, A.; Eskilsson, D.; Jaras, S. G. *Appl. Cat. B Environ.* **2007**, *69*, 240−251.

(33) Zheng, Y. J.; Jensen, A. D.; Johnsson, J. E. *Appl. Cat. B Environ.* **2008**, *83*, 186−194.

(34) Henriksson, M.; Warnqvist, B. *Ind. Chem. Process Des. Dev.* **1979**, *18*, 249−254.

(35) Fielder, W. L.; Stearns, C. A.; Kohl, F.J. *J. Electrochem. Soc.* **1984**, *131*, 2414−2417.

(36) Boonsongsup, L.; Iisa, K.; Frederick, W. J., Jr. *Ind. Eng. Chem. Res.* **1997**, *36*, 4212−4216.

(37) Nielsen, H. P.; Frandsen, F. J.; Dam-Johansen, K. *Energy Fuels* **1999**, *13*, 1114−1121.

(38) Nielsen, H. P.; Frandsen, F. J.; Dam-Johansen, K.; Baxter, L. L. *Prog. Energy Combust. Sci.* **2000**, *26*, 283−298.

(39) van Lith, S. C.; Frandsen, F. J.; Montgomery, M.; Vilhlemsen, T.; Jensen, S. A. *Energy Fuels* **2009**, *23*, 3457−3468.

(40) Paneru, M.; Maier, J.; Stein-Brzozowska, G.; Scheffknecht, G. Corrosion mechanism of alloy 310 austenetic steel beneath NaCl deposit under varying SO2 concentration in oxy-fuel combustion atmosphere. *Proceedings of the Impacts of Fuel Quality on Power Generation and the Environment*; Puchberg am Schneeberg, Austria, 2012.

(41) Uchida, S.; Kamo, H.; Kubota, H.; Kanaya, K. *Ind. Chem. Process Design Dev.* **1983**, *22*, 144−149.

(42) Uchida, S.; Kamo, H.; Kubota, H. *Ind. Eng. Chem. Res.* **1988**, *27*, 2188−2190.

(43) Warnqvist, R.; Norrström, H. *Tappi* **1976**, *59*, 89.

(44) Saint-Jean, S. J.; Jøns, E.; Lundgaard, N.; Hansen, S. *Cem. Concr. Res.* **2005**, *35*, 431−437.

(45) Ozawa, S.; Ito, K.; Matsuda, H. *Kagaku Kogaku Ronbunshu* **2002**, *28*, 396−403.

(46) Matsuda, H.; Ozawaa, S.; Narusea, K.; Itoa, K.; Kojimab, Y.; Yanasec, T. *Chem. Eng. Sci.* **2005**, *60*, 545−552.

(47) Arnold, H.; Kurtz, W.; Richterzinnius, A.; Bethke, J.; Heger, G. *Aacta Crystallogr. Sec. B Struct. Sci.* **1981**, *37*, 1643−1651.

(48) Bin Anooz, S.; Bertram, R.; Klimm, D. *Solid State Commun.* **2007**, *141*, 497−501.

(49) Jørgensen, T. L.; Livbjerg, H.; Glarborg, P. *Chem. Eng. Sci.* **2007**, *62*, 4496−4499.

(50) Lindberg, D.; Backman, R.; Chartrand, P. *J. Chem. Thermodyn.* **2006**, *38*, 1568−1583.

(51) Jensen, A.; Johnsson, J. E.; Dam-Johansen, K. *AIChE J.* **1997**, *43*, 3070−3084.

(52) Asta, M.; Beckermann, C.; Karma, A.; Kurz, W.; Napolitano, R.; Plapp, M.; Purdy, G.; Rappaz, M.; Trivedi, R. *Acta Mater.* **2009**, *57*, 941−971.

(53) Elliott, R. *Eutectic solidification processing: crystalline and glassy alloys*, Butterworths, 1983.